Supplementary Information (SI) for Journal of Materials Chemistry C.
This journal is © The Royal Society of Chemistry 2026

Supporting Information

Chirality-Guided Crystal Packing for Tunable Clustering-Triggered Emission

Zhipeng Zhao, Yueying Lai, Zhuojie Yin, Xiang Chen, Guangxin Yang, Junhao Duan, Yu Song Cai, Wang Zhang Yuan*

Experimental

Materials. *D*-valine (≥98.0%), *L*-valine (99%) were purchased from J&K Chemical Co., Ltd. Biscyclo[2.2.2]oct-7-ene-2,3,5,6-tetracarboxylic acid dianhydride (DA, ≥98.0%), glacial acetic acid (≥99.5%), and ether (analytical grade) were purchased from TCI Co., Ltd., Shanghai Aladdin Bio-Chem Technology Co., Ltd., and Shanghai Sino pharm Chemical Reagent Co., Ltd., respectively. The ultra-pure water was obtained from Hangzhou Wahaha Co., Ltd. DA was used after recrystallization, and other chemicals were used without further purification.

General methods. ^{1}H (500 MHz) and ^{13}C (126 MHz) NMR spectra were obtained on a Bruker AVANCE III-500 NMR spectrometer at room temperature using DMSO-d_6 as solvents and tetramethylsilane (TMS) as an internal reference. Circular dichroism (CD) absorption spectra were acquired with a circular dichroism spectrometer (J-1500, JASCO, Japan). Photoluminescence (PL) spectra and phosphorescence lifetimes of the solids were measured on an Edinburgh FSL1000 steady/transient fluorescence spectrometer, at room temperature or 77 K. The absolute quantum efficiencies (Φ) were measured on QM/TM/IM steady-state & time-resolved fluorescence spectrofluorometer (PTI, USA) equipped with a SPEKTRON-R98 coated integrating sphere (Φ 80 mm) (Everfine, China). Single crystal structures were examined on a

Bruker D8 Venture-CMOS Photon II X-ray diffractometer with helios mx multilayer monochrmator Cu Kα radiation (λ = 1.54178 Å). Data collection, unit cell refinement, and data reduction were performed using APEX3 v2019.11-0. The structure was solved by Intrinsic Phasing method and refined by full-matrix least-squares on F2 with anisotropic displacement parameters for the non-H atoms using SHELXTL program package. The hydrogen atoms on carbon were calculated in ideal positions with isotropic displacement parameters set to 1.2xUeq of the attached atom (1.5xUeq for methyl hydrogen atoms). The hydrogen atoms bound to nitrogen were located in a ΔF map and refined with isotropic displacement parameters. All photographs were taken by a digital camera (Sony α7sII, Japan). The monomer and dimer of the compounds used for theoretical calculation were extracted from their single crystal data. Time dependent density functional theory (TD-DFT) calculations were performed using Gaussian16 program (version A.03). The excitation energies and transition properties of the nth singlet state (S_n) and the nth triplet state (T_n) were obtained by using the B3LYP hybrid functional and 6-31+g(d,p) basis set.

Synthesis of the Compounds. As shown in Scheme S1, all compounds were facilely prepared by the amidation of DA with valine in glacial acetic acid under reflux.

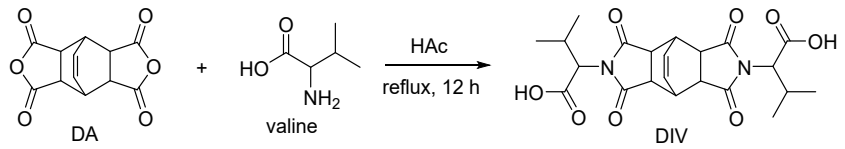

Scheme S1. Synthetic route to DIV.

Synthesis of *R*-DIV and *S*-DIV. Into a three-necked round bottom flask were placed DA (1.00 g, 4.03 mmol), *D*-valine or *L*-valine (944 mg, 8.06 mmol) and glacial acetic acid (35 mL). The mixture was stirred at room temperature until it became clear. Then it was heated to 130 ℃ and stirred for 12 h under reflux. Afterwards, the mixture was slowly cooled to room temperature. White solids were collected through flitration and washed with elthyl ether three times. The crude product was recrystallized in pure water and the resulting solids were collected and dired at 45 ℃ in oven overnight. *R*-DIV and

S-DIV crystals were obtained in 58.4% and 62.3% yields, respectively. *Characterization Data of R-DIV*: ^{1}H NMR (500 MHz, DMSO-d_6) δ (ppm) 12.81 (s, 2H), 6.05 (dd, J = 4.4, 3.1 Hz, 2H), 4.15 (d, J = 7.7 Hz, 2H), 3.43 (dt, J = 6.0, 3.1 Hz, 2H), 3.27 (t, 4H), 2.42–2.30 (m, 2H), 0.94 (d, J = 6.7 Hz, 6H), 0.68 (d, J = 6.8 Hz, 6H). ^{13}C NMR (126 MHz, DMSO-d_6) δ (ppm) 177.22, 169.51, 131.48, 57.67, 42.57, 33.82, 27.92, 21.28, 19.60. *Characterization Data of S-DIV*: ^{1}H NMR (500 MHz, DMSO-d_6) δ (ppm) 12.81 (s, 2H), 6.05 (dd, J = 4.4, 3.1 Hz, 2H), 4.15 (d, J = 7.8 Hz, 2H), 3.43 (dt, J = 6.1, 3.1 Hz, 2H), 3.27 (t, 4H), 2.44–2.30 (m, 2H), 0.94 (d, J = 6.7 Hz, 6H), 0.68 (d, J = 6.9 Hz, 6H). ^{13}C NMR (126 MHz, DMSO-d_6) δ (ppm) 177.28, 169.57, 131.54, 57.72, 42.62, 33.87, 27.97, 21.33, 19.65.

Synthesis of *rac*-DIV. The synthetic procedures of *rac*-DIV are similar to those described above for *R*-DIV and *S*-DIV by using DA (1.00 g, 4.03 mmol), *D*-valine (472 mg, 4.03 mmol) and *L*-valine (472 mg, 4.03 mmol) as the reactants. The resulting *rac*-DIV (1.23 g) was obtained in 68.5% yield. *Characterization Data of rac-DIV:* ^{1}H NMR (500 MHz, DMSO-d_6) δ (ppm) 12.81 (s, 2H), 6.05 (dd, J = 4.4, 3.1 Hz, 2H), 4.15 (d, J = 7.8 Hz, 2H), 3.43 (dt, J = 6.0, 3.1 Hz, 2H), 3.32 (t, 4H), 2.44–2.30 (m, J = 6.9 Hz, 2H), 0.94 (d, J = 6.7 Hz, 6H), 0.68 (d, J = 6.9 Hz, 6H). ^{13}C NMR (126 MHz, DMSO-d_6) δ (ppm) 176.82, 169.12, 131.24, 57.26, 42.23, 33.41, 27.51, 20.87, 19.19.

Figures and Tables

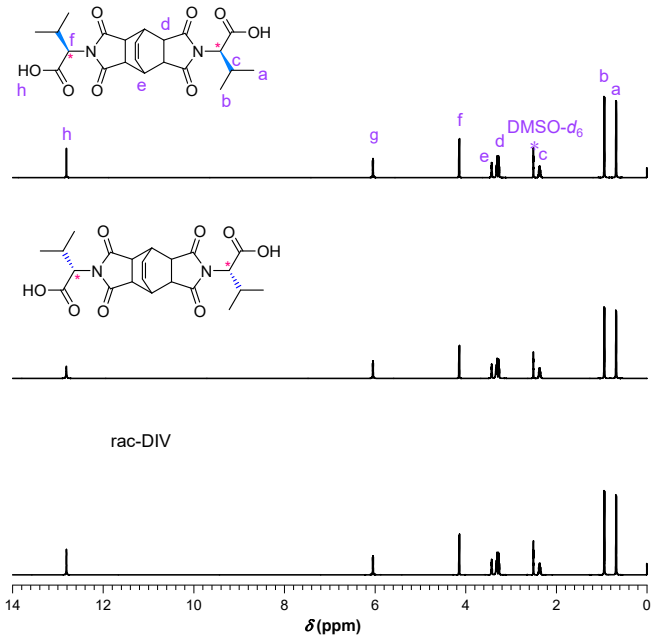

Fig. S1 ^{1}H NMR spectra of *R*-DIV, *S*-DIV, and *rac*-DIV in DMSO-d_6. The solvent peaks are marked with the asterisk.

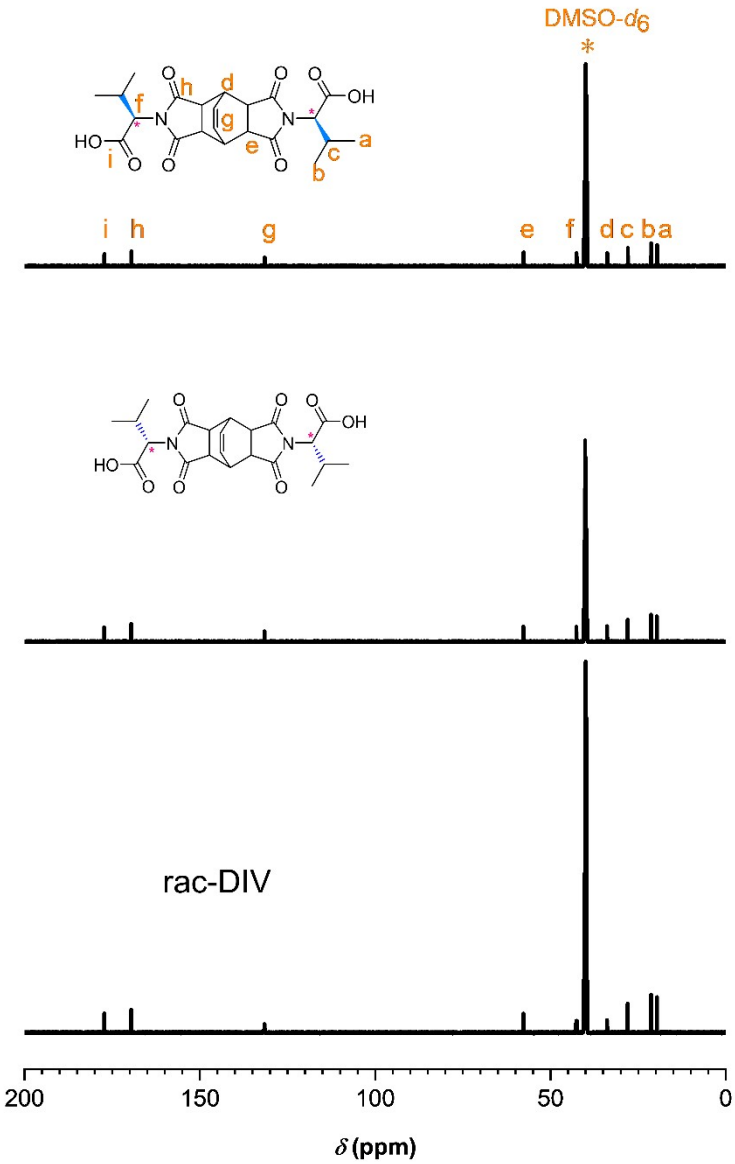

Fig. S2 ^{13}C NMR spectra of *R*-DIV, *S*-DIV and *rac*-DIV in DMSO-d_6. The solvent peaks are marked with the asterisk.

Table S1 Single crystal data of the compounds.

Compound	Space Group	Cell Length [Å]	Cell Angle [°]	Cell Volume [Å^3]	Z	Density [g cm^{-3}]
R-DIV	Monoclinic P2(1)	a = 6.6702(4) b = 30.9085(19) c = 10.7258(6)	α = 90 β = 90.911(3) γ = 90	2211.0 (2)	4	1.341
S-DIV	Triclinic P1	a = 6.9137(14) b = 12.487(2) c = 13.497(3)	α = 101.771(16) β = 93.73(2) γ = 96.212(15)	1129.5 (4)	2	1.366
rac-DIV	Monoclinic C2/c	a = 23.824(12) b = 7.078(6) c = 13.438(6)	α = 90 β = 112.90(4) γ = 90	2088.0(2)	4	1.420

Note: *S*-DIV contains lattice water.

Table S2 Crystal data and structure refinement for *R*-DIV

Identification code	*R*-DIV
Empirical formula	$C_{22}H_{26}N_2O_8$
zFormula weight	446.45
Temperature/K	297(2)
Crystal system	Monoclinic
Space group	$P2_1$
a/Å	6.6702(4)
b/Å	30.9085(19)
c/Å	10.7258(6)
α/°	90
β/°	90.911(3)
γ/°	90
Volume/Å^3	2211.0(2)
Z	4
ρcalcg/cm^3	1.341
μ/mm^{-1}	0.863
F(000)	944
Crystal size/mm^3	0.180 × 0.160 × 0.150
Radiation	Cu Kα (λ = 1.54178)
2Θ range for data collection/°	4.122 to 66.567
Reflections collected	15904
Data/restraints/parameters	7511/1/601
Goodness-of-fit on F^2	1.032
Final R indexes [I>=2σ (I)]	R1 = 0.0572, wR2 = 0.1536
Final R indexes [all data]	R1 = 0.0655, wR2 = 0.1674
Largest diff. peak/hole / e Å^{-3}	0.692/-0.241

Table S3 Crystal data and structure refinement for *S*-DIV·H_2O

Identification code	*S*-DIV·H_2O
Empirical formula	$C_{22}H_{28}N_2O_9$
zFormula weight	464.46
Temperature/K	297(2)
Crystal system	Triclinic
Space group	*P*1
a/Å	6.9137(14)
b/Å	12.487(2)
c/Å	13.497(3)
α/°	101.771(16)
β/°	93.73(2)
γ/°	96.212(15)
Volume/Å^3	1129.5(4)
Z	2
ρcalcg/cm^3	1.366
μ/mm^{-1}	0.899
F(000)	492
Crystal size/mm^3	0.220 ×0.180 ×0.160
Radiation	Cu Kα (λ = 1.54178)
2Θ range for data collection/°	4.400 to 66.870
Reflections collected	12598
Data/restraints/parameters	7182/3/632
Goodness-of-fit on F^2	1.018
Final R indexes [I>=2σ (I)]	R1 = 0.0505, wR2 = 0.1392
Final R indexes [all data]	R1 = 0.0605, wR2 = 0.1511
Largest diff. peak/hole / e Å^{-3}	0.525/-0.312

Table S4 Crystal data and structure refinement for *rac*-DIV

Identification code	*rac*-DIV
Empirical formula	$C_{22}H_{28}N_2O_9$
zFormula weight	446.45
Temperature/K	297(2)
Crystal system	Monoclinic
Space group	*C2/c*
a/Å	23.824(12)
b/Å	7.078(6)
c/Å	13.438(6)
α/°	90
β/°	112.90(4)
γ/°	90
Volume/Å^3	2088(2)
Z	4
ρcalcg/cm^3	1.420
μ/mm^{-1}	0.109
F(000)	944
Crystal size/mm^3	0.470 ×0.100 ×0.100
Radiation	Mo Kα (λ = 0.71073)
2Θ range for data collection/°	1.856 to 25.390
Reflections collected	8583
Data/restraints/parameters	1921/0/148
Goodness-of-fit on F^2	1.037
Final R indexes [I>=2σ (I)]	R1 = 0.0560, wR2 = 0.1570
Final R indexes [all data]	R1 = 0.0670, wR2 = 0.1719
Largest diff. peak/hole / e Å^{-3}	0.437/-0.389

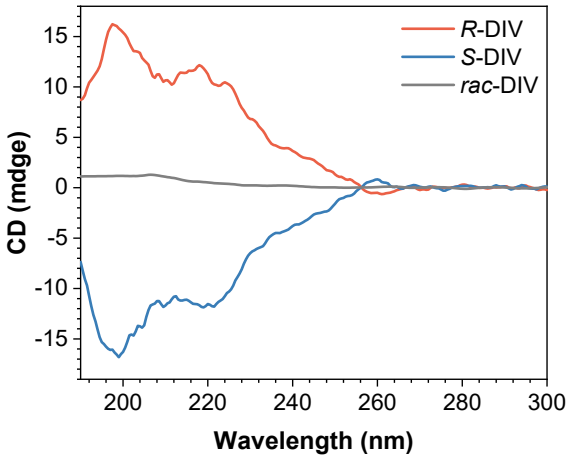

Fig. S3 CD absorption spectra of enantiomers and racemates.

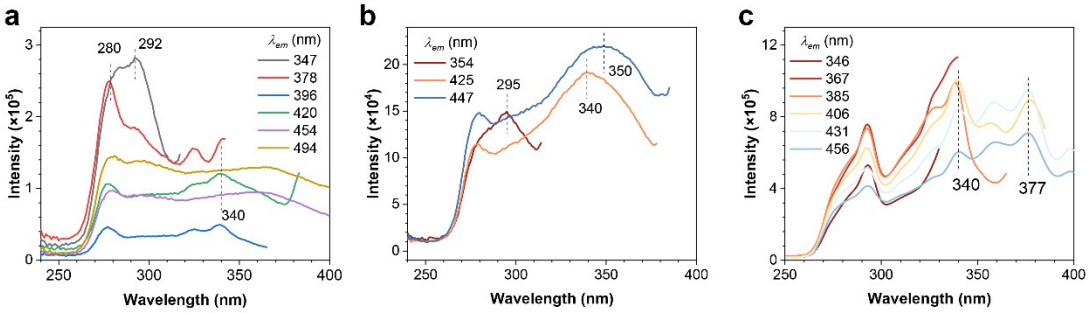

Fig. S4 The excitation spectra of *R*-DIV(a), *S*-DIV(b) and *rac*-DIV(c) at room temperature.

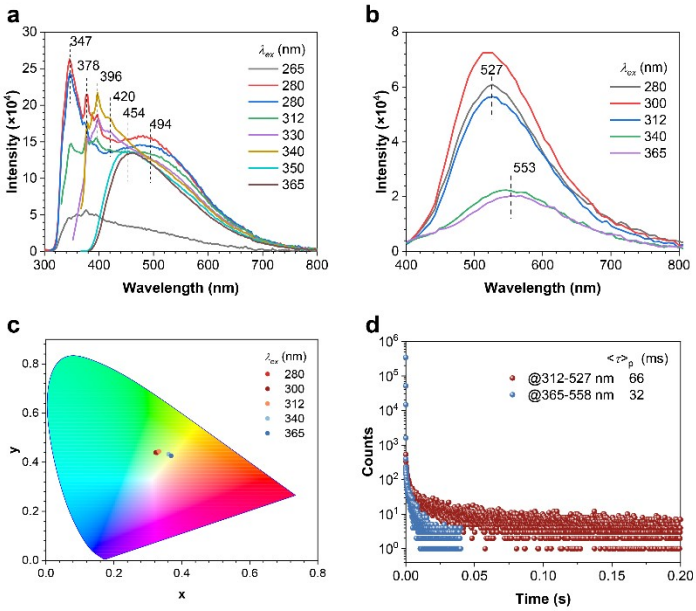

Fig. S5 (a) Prompt PL spectra and (b) delayed (t_d = 1 ms) PL spectra of *R*-DIV at room

temperature under varying excitation wavelengths. (c) The CIE coordinates corresponding to the delayed spectra and (d) the phosphorescence decay curves.

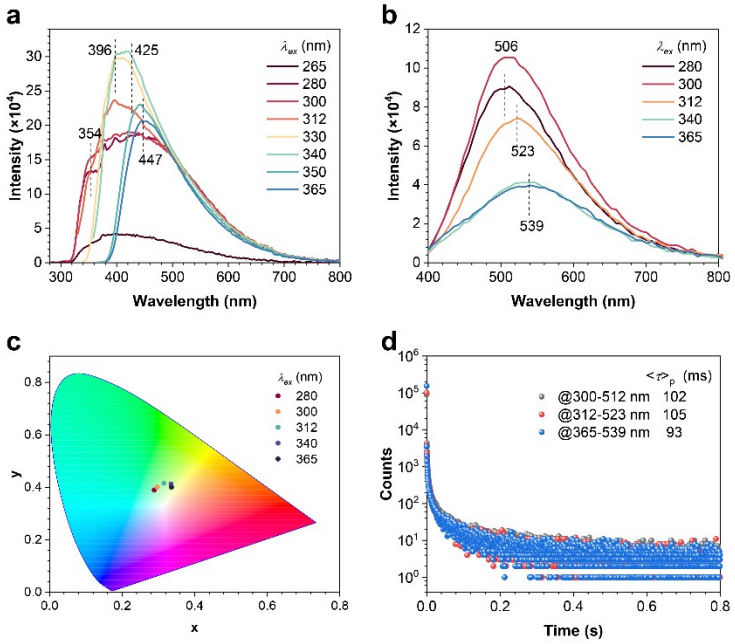

Fig. S6 (a) Prompt PL spectra and (b) delayed (t_d = 1 ms) PL spectra of *S*-DIV at room temperature under varying excitation wavelengths. (c) The CIE coordinates corresponding to the delayed spectra and (d) the phosphorescence decay curves.

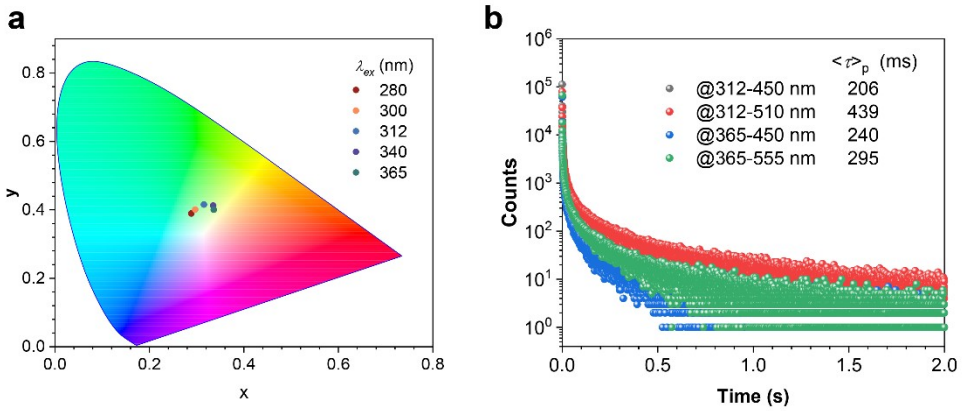

Fig. S7 (a) CIE chromaticity coordinates derived from the delayed PL spectra and (b) phosphorescence decay curves of *rac*-DIV crystals at room temperature.

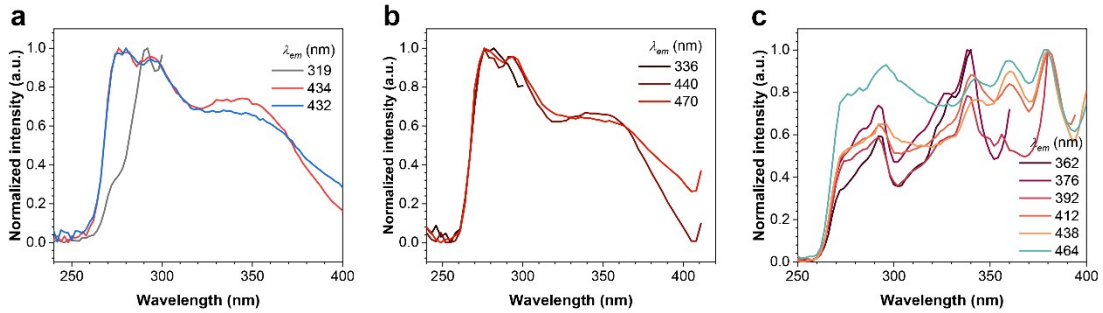

Fig. S8 The excitation spectra of *R*-DIV(a), *S*-DIV(b) and *rac*-DIV(c) at 77 K.

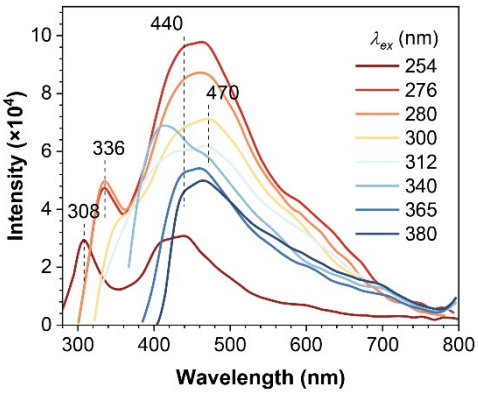

Fig. S9 Prompt PL spectra of *R*-DIV at 77 K under varying excitation wavelengths.

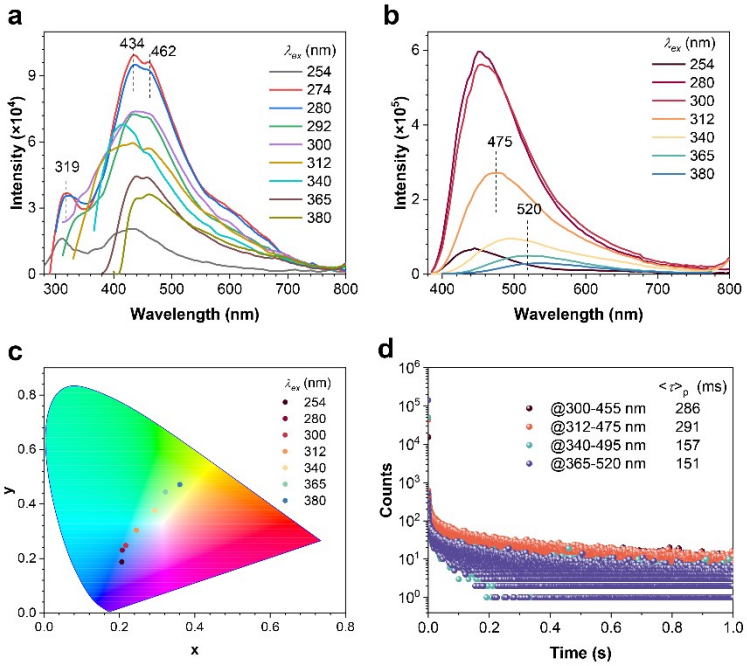

Fig. S10 (a) Prompt PL spectra and (b) delayed (t_d = 1 ms) PL spectra of *S*-DIV at 77 K under varying excitation wavelengths. (c) The CIE coordinates corresponding to the delayed spectra and (d) the phosphorescence decay curves.

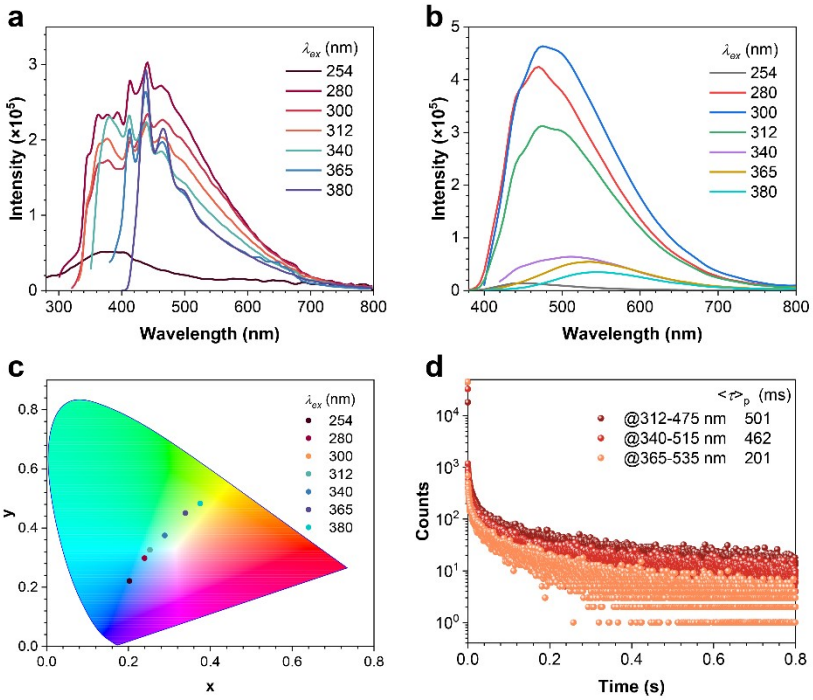

Fig. S11 (a) Prompt PL spectra and (b) delayed (t_d = 1 ms) PL spectra of *rac*-DIV at 77 K under varying excitation wavelengths. (c) The CIE coordinates corresponding to the delayed spectra and (d) the phosphorescence decay curves.

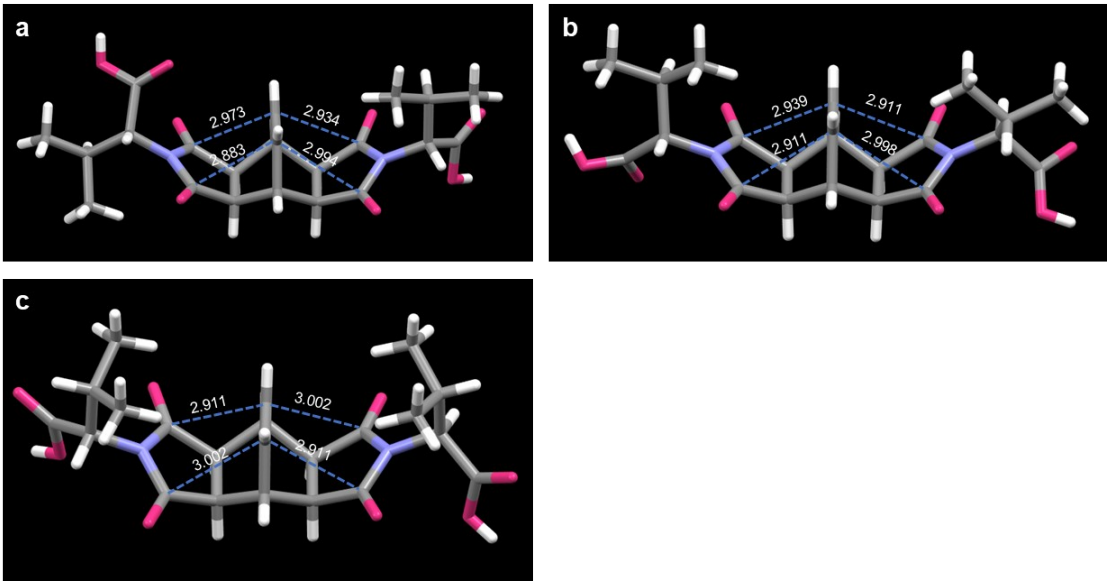

Fig. S12 O=C···C=C interactions in *R*-DIV (a), *S*-DIV (b), and *rac*-DIV (c) crystals.

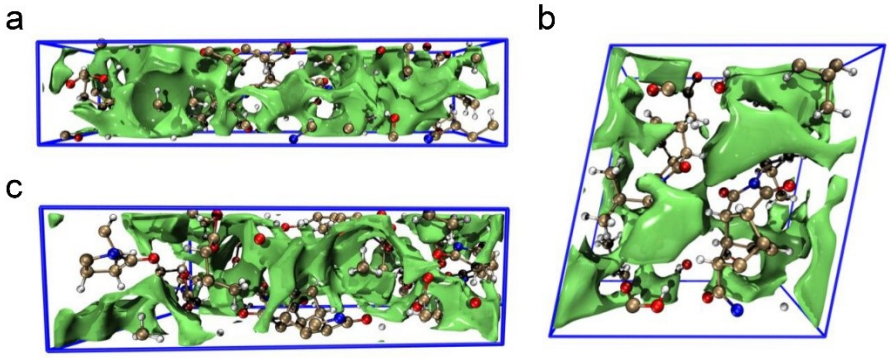

Fig. S13 Visual representation of the free volume (green isosurfaces) in the unit cells of (a) *R*-DIV, (b) *S*-DIV, and (c) *rac*-DIV.

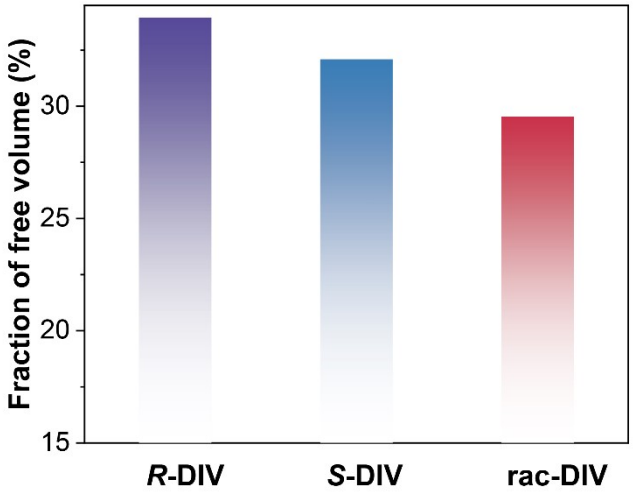

Fig. S14 Comparison of the calculated free volume percentages in the crystal lattices of *R*-DIV, *S*-DIV, and *rac*-DIV.

Author contributions

Z.Z., Y.L. and W.Z.Y. conceived the study. Z.Z. and Y.L. conducted the experiments. Z.Y., C.C., G.Y., J.D. and Y.S.C. provided support to Z.Z. and Y.L. for the experiments. Z.Z. and W.Z.Y. discussed the results and wrote the manuscript.